HHS Public Access

Author manuscript

J Physiol. Author manuscript; available in PMC 2020 August 01.

Published in final edited form as:

J Physiol. 2019 August ; 597(15): 3817–3832. doi:10.1113/JP277769.

MitoBK$_{Ca}$ channel is functionally associated with its regulatory β1 subunit in cardiac mitochondria

Enrique Balderas[6], **Natalia S. Torres**[6], **Manuel Rosa-Garrido**[1,2], **Dipayan Chaudhuri**[6], **Ligia Toro**[1,3,4,5], **Enrico Stefani**[1,2,3,5], **Riccardo Olcese**[1,2,3,5]

[1]Dept. of Anesthesiology & Perioperative Medicine, Division of Molecular Medicine, David Geffen School of Medicine, University of California at Los Angeles, Los Angeles, CA, 90095, USA

[2]Dept. of Physiology, David Geffen School of Medicine, University of California at Los Angeles, Los Angeles, CA, 90095, USA

[3]Cardiovascular Research Laboratories, David Geffen School of Medicine, University of California at Los Angeles, Los Angeles, CA, 90095, USA

[4]Dept. of Molecular and Medical Pharmacology, David Geffen School of Medicine, University of California at Los Angeles, Los Angeles, CA, 90095, USA

[5]Brain Research Institute, David Geffen School of Medicine, University of California at Los Angeles, Los Angeles, CA, 90095, USA

[6]Nora Eccles Harrison Cardiovascular Research & Training Institute, University of Utah, Salt Lake City, UT. 84112, USA

Abstract

Association of plasma membrane BK$_{Ca}$ channel with auxiliary BK-β (1–4) subunits profoundly affects regulatory mechanisms and physiological processes in which this channel participate. However, functional association of mitochondrial BK (mitoBK$_{Ca}$) with regulatory subunits is unknown. We report that mitoBK$_{Ca}$ functionally associates with its regulatory subunit BK-β1 in adult rodent cardiomyocytes. Cardiac mitoBK$_{Ca}$ is a calcium and voltage activated channel, sensitive to paxilline with a large conductance for K^+ of 300 pS. Additionally, mitoBK$_{Ca}$ displays a high open probability (P_o) and voltage half of activation ($V_{1/2}$ = −55 mV, n=7) that resembles that of plasma membrane BK$_{Ca}$ when associated with its regulatory BK-β1 subunit. Immunochemistry assays demonstrated an interaction between mitochondrial BK$_{Ca}$-α and its BK-β1 subunit. Mitochondria from the BK-β1 KO mice showed sparse mitoBK$_{Ca}$ currents (5 patches

Correspondence to: Enrique Balderas Ph.D., Nora Eccles Harrison Cardiovascular Research & Training Institute, The University of Utah, Salt Lake City, UT., u6010182@utah.edu.

Author contributions

E.B.: experimental design and project conception, electrophysiology, calcium retention capacity measurements, confocal imaging and immunofluorescence experiments, analysis and interpretation of data, writing of manuscript; N.T.: immunochemistry assays experimental design and interpretation of data, writing of manuscript; M.R-G. qRT-PCR experiments and analysis; D.C., L.T., E.S, and R. O.: experimental design, project conception, interpretation of data and manuscript writing. All authors have read and approved the final version of this manuscript and agree to be accountable for all aspects of the work in ensuring that questions related to the accuracy or integrity of any part of the work are appropriately investigated and resolved. All persons designated as authors qualify for authorship, and all those who qualify for authorship are listed.

Competing interests

The authors declare no competing financial interests.

with mitoBK$_{Ca}$ activity out of 28 total patches from n=5 different hearts), displaying a depolarized $V_{1/2}$ activation (+47 mV in 12 μM matrix Ca^{2+}). The reduced activity of mitoBK$_{Ca}$ was accompanied with a high expression of BK$_{Ca}$ transcript in the BK-β1 KO, suggesting less abundance of mitoBK$_{Ca}$ channels in this genotype. Accordingly, BK-β1subunit increased two-fold the localization of BKDEC (the splice variant of BK$_{Ca}$ that specifically targets mitochondria) into mitochondria. Importantly, both paxilline treated and BK-β1 KO mitochondria displayed a more rapid Ca^{2+} overload, featuring an early opening of the mitochondrial transition pore (mPTP). We provide strong evidence that mitoBK$_{Ca}$ associates with its regulatory BK-β1 subunit in cardiac mitochondria, ensuring proper targeting and activation of the mitoBK$_{Ca}$ channel helps to maintain mitochondrial Ca^{2+} homeostasis.

Keywords

cardiomyocytes; mitochondria; potassium channel; Paxilline; mitochondrial calcium retention capacity

Introduction

Large conductance for K^+, voltage and Ca^{2+}-activated channels (Slo1, MaxiK, BK$_{Ca}$) are expressed at the plasma membrane of a wide variety of cell types and tissues (Latorre & Brauchi, 2006; Salkoff *et al.*, 2006; Cui *et al.*, 2009a; Berkefeld *et al.*, 2010; Latorre *et al.*, 2010; Lee & Cui, 2010a; Contreras *et al.*, 2013; Hoshi *et al.*, 2013). BK$_{Ca}$ activity governs cellular excitability, Ca^{2+} homeostasis, signaling cascades and neurotransmitter release (Lancaster & Nicoll, 1987; Meredith *et al.*, 2006; Cui *et al.*, 2009b; Lee & Cui, 2010b). In the cardiovascular system, the activity of BK$_{Ca}$ channels regulates vascular tone and blood pressure (Brayden & Nelson, 1992; Ledoux *et al.*, 2006). In adult cardiomyocytes, BK$_{Ca}$ channels are targeted almost exclusively to the inner mitochondrial membrane (Singh *et al.*, 2013; Balderas *et al.*, 2015) where their activation exerts a cardioprotective effect (Xu *et al.*, 2002; Sato *et al.*, 2005; Singh *et al.*, 2013; Soltysinska *et al.*, 2014). While the biophysical properties of plasma membrane BK$_{Ca}$ (i.e. voltage dependence, Ca^{2+}-sensitivity and gating) depend on their interactions with auxiliary β and γ subunits (Latorre *et al.*, 2017), the expression of the auxiliary BK-β1 subunit in cardiac mitochondria has been demonstrated by two independent groups (Ohya *et al.*, 2005; Bautista *et al.*, 2009). However, the functional association of BK$_{Ca}$ channels with its regulatory BK-β1 subunits in cardiac mitochondria has yet to be determined.

An initial characterization of mitoBK$_{Ca}$ channels by the O'Rourke laboratory revealed a K^+ conductance of ~300 pS in cardiac mitoplast-attached patches; this channel was also found to be sensitive to changes in mitochondrial Ca^{2+} and inhibited by Charybdotoxin (CTx) when applied into the patch pipette (Xu *et al.*, 2002). These results, together with Siemen's pioneering work in a glioma cell line LN229, established that mitoBK$_{Ca}$ shares key properties, such as large conductance for K^+ and sensitivity to voltage and Ca^{2+} (Siemen *et al.*, 1999), with the plasma membrane BK$_{Ca}$ (Barrett *et al.*, 1981; Latorre *et al.*, 1982; Latorre *et al.*, 1989). The conductance of mitoBK$_{Ca}$ varies among different tissues and cell types, however several laboratories have reported a conductance between 200 and 550 pS for

mitoBK$_{Ca}$ as recently reviewed by our group (Singh *et al.*, 2012; Balderas *et al.*, 2015). A conductance of 145 pS for cardiac mitoBK$_{Ca}$, slightly smaller to the commonly reported conductance for mitoBK$_{Ca}$ and the one reported in the present work was recently reported (Frankenreiter *et al.*, 2017) (see discussion). Current findings indicate rodent cardiac mitoBK$_{Ca}$ is a splice variant of plasma membrane BK$_{Ca}$ (*Kcnma1*) containing an extra 50 amino acids at the end of the C-terminus (the "DEC" sequence) essential to target BK$_{Ca}$ to the mitochondria in adult cardiomyocytes (Singh *et al.*, 2013). Hearts exposed to BK$_{Ca}$ openers NS1619 (Xu *et al.*, 2002; Stowe *et al.*, 2006; Singh *et al.*, 2013), NS11021 (Bentzen *et al.*, 2010), and Naringenin (Testai *et al.*, 2013) reduced infarct size in ischemia-reperfusion assays, whereas mice hearts lacking BK$_{Ca}$ (*Kcnma1−/−*) were not protected (Singh *et al.*, 2013; Soltysinska *et al.*, 2014; Frankenreiter *et al.*, 2017). The cardioprotective effect of opening mitoBK$_{Ca}$ has been linked to the capacity of mitochondria to tolerate Ca^{2+} loading (Sato *et al.*, 2005; Stowe *et al.*, 2006; Singh *et al.*, 2013).

Despite of the growing evidence for a role of mitoBK$_{Ca}$ channels in mitochondrial and heart physiology, their voltage-dependence and association with regulatory BK-β subunits are unknown. We identify a population of mitoBK$_{Ca}$ channels in adult rodent cardiomyocytes with high voltage sensitivity. Molecular and immunochemistry analyses indicate that such a characteristic arises from the association of mitoBK$_{Ca}$ with its regulatory β1 subunit. In addition a second population of mitoBK$_{Ca}$ channels with a more depolarized voltage dependency of activation ($V_{1/2}$= +40 mV at 12 μM matrix Ca^{2+}, n=7) was identified, suggesting a different subunit composition.

Materials and Methods

Ethical approval

The animal protocols were approved by the Institutional Animal Care and Use Committee (IACUC). At UCLA, animal care and use program is guided by federal and state laws, regulations, and guidelines, and by additional institutional policies implemented to systematically address federal requirements and as the result of a voluntary accreditation process. The Public Health Service Policy on Humane Care and Use of Animals (PHS Policy) and USDA Animal Welfare Regulations (AWRs) provide the primary regulatory basis for the existence and function of the IACUC.

The authors understand, and the work conforms to, the principles and regulations of *The Journal of Physiology* (Grundy, 2015).

Animals.—Sprague-Dawley male rats (3 months old), and three-month-old wild type (C57BL/6NCrL, Charles River laboratories) and β1 KO (β1$^{-/-}$) male mice were raised in the animal facilities at UCLA. Animals were housed in a 12h light-dark cycle with *ad libitum* access to food and water. Animals were euthanized by an overdose of pentobarbital sodium.

The BK-β1 KO (*kcnmb1−/−)* line was generated in the laboratory as described in a previous publication (Li *et al.*, 2013).

Antibodies.—Polyclonal antibody against BK_{Ca} (Rabbit Anti-KCNMA1 Cat. APC-021 and APC-151), and polyclonal antibody for BK-β1 subunit (Rabbit Anti-KCNMB1, Cat. APC-036) were from Alomone labs. Monoclonal antibody against GRIM19 (Mouse Ab110240) was from Abcam. Polyclonal antibody against SERCA (Rabbit, Anti-ATP2A2/SERCA2 cat. 4388) was from Cell Signaling. Alexa Fluor 555® anti-goat and anti-rabbit (A21428), and anti-donkey and anti-mouse (A28180) were from Invitrogen. Anti-HA monoclonal antibody (Ab. H3663), and Anti-Flag polyclonal antibody (Ab. F7425) were from Sigma.

Isolation of left ventricle cardiomyocytes (LVC)

Adult male Sprague Dawley rats (3 months old) were injected intraperitonealy (i. p.) with heparin (200 IU/kg). After 20 min, animals were euthanized with single dose of pentobarbital sodium (60 mg/kg) (i. p.) followed by cervical dislocation. The heart was surgically removed and arrested immediately on ice-cold PBS solution (in mM: KCl 2, KH_2PO_4 1.5, NaCl 138, and Na_2HPO_4 8.1), the surrounding vasculature tissue was removed followed by quick aortic cannulation on a modified Langendorff apparatus. Hearts were perfused for 5 min with Tyrode's solution (in mM: NaCl 130, KCl 5.4, $MgCl_2$ 1, Na_2HPO_4 0.6, glucose 10, taurine 5, 2, 3-butanedione monoxime 10, and HEPES 10, pH 7.4, oxygenated with 95% (*v/v*) O_2, 5% (*v/v*) CO_2, 37°C) at a constant pressure of 80 cm H_2O. Once all the internal blood was rinsed out, the hearts were digested by enzyme perfusion with Tyrode's solution supplemented with 372 U/ml Collagenase Type-2 and 1.0 U/ml Protease Type-XIV. After 15–20 min, the enzymatic solution was substituted with oxygenated Krebs buffer (KB) (in mM: KCl 25, KH_2PO_4 10, $MgSO_4$ 2, Glucose 20, Taurine 20, Creatinine 5, K-Glutamate 100, Aspartic acid 10, EGTA 0.5, HEPES 5, and 1% (*w/v*) BSA, pH 7.2). After 10 min hearts were dismounted and washed on ice cold KB solution to remove the right ventricle and the vascular tissue. The left ventricle was manually dissociated and cardiomyocytes were released into the KB solution. Isolated cardiomyocytes were filtered through a 100 μm mesh and centrifuged at 1000 x*g* for 60 s in KB buffer.

All the experiments were performed according to NIH guidelines and received ethical approval from the UCLA Office of Animal Research Oversight (OARO).

Labeling cardiomyocytes with Mitotracker red

Freshly dissociated cardiomyocytes were incubated with 200 nM Mitotracker red (Invitrogen) for 15 min at 37°C. The excess of Mitotracker red was removed with KB buffer.

Isolation of mitochondria from LVC

Cardiomyocytes were suspended in isolation buffer "A" (in mM: 230 Mannitol, 70 sucrose, 10 HEPES, 2 EDTA, pH 7.2 supplemented with 1 mg/ml fatty acid-free BSA), loaded into a cold glass potter and gently homogenized on ice (up to 10 strokes). The homogenate was recovered and centrifuged at low speed (1,300 x*g* 4°C) for 5 min. The supernatant was collected and centrifuged at high speed (10,000 x*g* 4°C) for 10 min. Isolated mitochondria were maintained on ice.

Mitoplast preparation

Isolated mitochondria were resuspended in 2 ml hypotonic buffer “B” (in mM: 5 HEPES, 2 EDTA, pH 7.2) and shaken on ice for 12 min. After this time, samples were centrifuged for 5 min at 12,500 rpm 4°C. The pellet (mitoplasts: mitochondrial internal membrane stripped of outer membrane, was dissolved in isotonic buffer “C” (in mM: 150 KCl, 5 HEPES, pH 7.2.) and stored at 4°C for further usage.

Electrophysiology and analysis

Mitoplasts were placed into a recording chamber filled with bath solution (in mM: 140 $KMeSO_3$, 10 KCl, 5 HEPES, pH 7.4. Only those mitoplasts that showed mitotracker red signal were used for patch-clamp. The concentration of free Ca^{2+} was calculated with MaxChelator (Stanford University), [Ca^{2+}] was controlled with EGTA or HEDTA and measured with a calcium electrode (World Precision Instruments). Borosilicate glass microelectrodes (~25 MΩ) filled with pipette solution (in mM: 140 $KMeSO_3$, 10 KCl, 5 HEPES, pH 7.4) were approached to the mitoplast until a high resistance seal (>5 GΩ) was formed. Recordings were performed within ~48 h after preparation of mitoplasts using the inside-out patch configuration. The membrane potential was clamped with an Axopatch 200A amplifier (Molecular Devices, Sunny Valley CA) controlled with a custom made software (G-patch). Single channel recordings were acquired at 5 kHz, filtered at 1 kHz and digitized through an analog/digital interface connected to a PC. Data analysis was performed with QuB software (SUNY Buffalo). NP_o was determined from total point amplitude histograms by measuring the fraction of time (Pk) spent at each open level (k) using a half amplitude criteria and summing the contributions of each channel $NPo = \sum kPk$Data points of NP_o were normalized to the NP_o max at +80 mV in 12 μM Ca^{2+} and plotted as a function of voltage (V). The half activation potential ($V_{1/2}$) was estimated by fitting NP_o data with a Boltzmann equation

$$\left\{1 + exp\left[-z\left(V - V_{1/2}\right)/kT\right]\right\}^{-1}$$

where V is the command pulse (mV), $V_{1/2}$ is the half voltage of activation and z the slope value, k the Boltzman constant, T the absolute temperature. Bars represent SEM with a minimum of 3 different experiments and p values were obtained by performing two tailed Student’s t-test.

Co-immunoprecipitation

Isolated cardiac mitochondria were harvested and solubilized with ice-cold RIPA buffer supplemented with protease and phosphatase inhibitors (4,000 and 6,000 μg/ml, respectively) (100x, Cell Signaling cat # 5872). Protein G magnetic beads (100 μl, SureBeads™, Biorad) were washed and saturated with specific polyclonal antibody (4 μg BK_{Ca} Ab-Alomone, APC-021) and pre-incubated with 500 μl (2 mg protein) of precleared lysate for 1 h at room temperature. Beads were washed 3 times with PBS-T (PBS-0.1% Tween 20) and eluted in 40 μl of 1x Laemmli buffer (Biorad) by incubating for 10 minutes at 70°C. Total and mitochondrial fraction lysates, and immunoprecipitated proteins were analyzed on a 4–20% SDS-polyacrylamide gel and transferred onto 0.2 μm PVDF

membrane. Western blots were probed with primary antibodies anti-BK_{Ca} (Alomone APC-151, 1:100), and anti-BK-β1 subunit (Alomone APC-036, 1:200). For control blots the membranes were striped and re-blotted with anti-SERCA (Cell Signaling 4388, 1:1000) and anti-GRIM19 (Abcam ab110240, 1:1000), and revealed by immunofluorescence using either goat anti-rabbit Alexa Fluo 555® (Invitrogen A21426, 1:5,000) or donkey anti-mouse AlexaFluo 555® (Invitrogen, 1:10,000) and a Chemidoc system (Biorad). Signal of the BK-β1 subunit in the whole lysate was detected with primary antibody against BK-β1 (APC-036, Alomone) 1:200, at 4°C on a rocker. Secondary antibody: goat anti rabbit-HRP (Jackson, 111-035-144) 1:10000, incubated for 1 h at room temperature on a rocker. Detection was performed with chemiluminescent (ECL) substrate Super Signal™ West Femto Maximum Sensitivity (Thermo, 34095), and imaged with Chemidoc system (Biorad).

Real-time quantitative PCR

Total RNA was purified from isolated adult mice (C57BL/6NCrL) cardiomyocytes lysed with TRIzol (Ambion, 15596018). RNA samples were digested for 10 min at room temperature with RNase-free DNase and cleaned-up with RNeasy mini kit (Qiagen). cDNA was synthesized using 0.5 μg of cleaned RNA following the provided instructions of the iScript cDNA Synthesis Kit (Bio-Rad, 170–8891). qPCR was performed using SsoFast EvaGreen Supermix (Bio-Rad, 172–5201) on a BioRad C1000 thermocycle. Primers used are detailed in Table S1. PCR was performed as follows: 98°C for 2min; [98°C for 5 sec; 60°C 5 sec] 60 cycles; for real time Melting curve [65°C for 5 sec increasing by half a degree each cycle until 95°C]. As control we used primers of glyceraldehyde 3-phosphate dehydrogenase (GAPDH, see Table 1). All samples are from duplicates and were normalized using the comparative Delta Delta Ct (ΔΔCt) method.

Transient transfection of HeLa cells

HeLa cells were seeded on 25 mm circle coverslips (0.13 mm thick, Fisher Scientific, Pittsburg, PA) coated with 0.1% (v/v) laminin (Sigma) in PBS and cultured in DMEM medium supplemented with 10% (v/v) FBS and antibiotics. When a confluence of >60% was reached cells were transfected. Transfection was performed with Lipofectamine 2000 (Invitrogen) following the protocol provided by the manufacturer. Briefly, cells incubated in presence of cDNA-Lipofectamine 2000 complexes (in 1:3 ratios) in Opti-MEM media (Invitrogen). One group of cells was transfected with the clone of full length human α subunit of BK-DEC channel alone, this construct includes the splice insert DEC sequence (EKKWFTDEPDNAYPRNIQIKPMSTHMANQINQYKSTSSLIPPIREVE**DEC**) at the C-terminus. A second group of cells was co-transfected with both HA tagged-BK_{Ca} DEC and Flag-human β1 subunit in a 1:3 cDNA ratio. Cells transfected with empty vector were used as negative control (MOCK). Transfection was stopped after 6 h. Cells were incubated for 72 h at 37°C.

Immunolabeling

After 72 h of transfection, slides were loaded with 200 nM Mitotracker red CMXRos incubated for 15 min at 37°C followed by three washes with PBS. Cells were fixed with 4% paraformaldehyde (15 min at room temperature) followed by three washes with PBS.

Samples were permeabilized with 0.5% (v/v) Triton-X 100 in PBS (10 min at RT). Nonspecific binding of the antibodies was prevented by incubation of cells in 5% (v/v) Normal Goat Serum (NGS, Jackson Immuno Research) in 2% BSA (Sigma) diluted in PBS 0.5% (v/v) Triton-X 100 for 30 min at room temperature. After this time, cells were incubated overnight at 4°C with specific primary antibodies AntiHA mAb, AntiFlag pAb diluted in PBS containing 0.5% Triton-X 100, 0.5% NGS, and 0.2% BSA. After washing the cells three times with PBS 0.5% Triton X-100 the slides were incubated for 60 min at RT with conjugated secondary antibodies Atto-647N (1 μg/ml anti mouse) and Alexa-488 (1 μg/ml) diluted in PBS containing 0.5% Triton-X 100, 0.5% NGS, and 0.2% BSA. Slides were mounted with ProLong Gold (Invitrogen). Confocal images (Fig. 5) were acquired with a Nikon Confocal microscope using a 60X oil immersion objective with 1.42 NA (Plan Apo) at scanning resolution of 0.27 μm/pixel. Sequential confocal images of HeLa cells were acquired from the same field. Images were median filtered (median intensities of 32 X 32-pixel squares centered at the target pixel were subtracted from the target pixel) and analyzed using a custom built software to determine the Cross correlation index (Cci) (Li *et al.*, 2010; Wu *et al.*, 2010).

Mitochondrial Calcium Retention Capacity (mCRC)

Freshly isolated mice cardiac mitochondria was gently dissolved in ice-cold buffer “C” (in mM, Sucrose 150, KCl 50, KH_2PO_4 2, Succinic Acid 5, Tris 20, pH 7.4 HCl). Basal fluorescence was measured in buffer “C” without mitochondria using a Fluorolog-3 (HORIBA LTD). Calcium green-5N (500nm excitation, 530nm emission) reports the Ca^{2+} content of the extra mitochondrial media. When mitochondria were added to the cuvette a sudden drop in fluorescence was recorded due to a lower transmittance of the solution and mitochondrial Ca^{2+} uptake. The signal stabilized in ~90 s. After this time, normoxic mitochondria were challenged with pulses of 10 nmol $CaCl_2$ applied every 60 s. CRC was defined as the total amount of Ca^{2+} added until the mitochondrial permeability transition pore (mPTP) opened. Recordings were normalized to the maximum fluorescence recorded before the addition of mitochondria (F/Fmax). Values of CRC were expressed as nmol of Ca^{2+}/mg mitochondrial protein.

RESULTS

Developing a method to purify intact mitoplasts for patch-clamp recording.

Mitochondria represent more than 30% of cell volume in adult cardiomyocytes. We purified mitochondria from rat left ventricle cardiomyocytes (Fig. 1A). The outer mitochondrial membrane was disrupted by hypotonic shock and the mitoplasts were recovered. Micrographs of fixed mitoplasts (2% polyethylene glycol) show the integrity of the purified mitoplasts. This method yielded a highly enriched mitoplast preparation (Fig. 1B). Only mitoplasts displaying Mitotracker red signal (Fig. 1C) were used for voltage-clamp (arrow in Fig. 1C, D). Only excised inside-out mitochondrial patches were used in this study. Inside-out configuration was achieved by pulling out the patch pipette after Giga seal (>10 GΩ) formation. Inside-out configuration was interpreted as the matrix side of the mitochondria exposed to the bath solution (Fig. 1E). In those patches were the inside-out configuration

was not achieved the activity of mitoBK$_{Ca}$ channel was not observed even at high Ca^{2+} (>10 μM) in the bath solution.

Cardiac mitochondrial inner membrane expresses a large conductance, voltage- and Ca^{2+}-dependent channel with a relatively high P_o: mitoBK$_{Ca}$.

We characterized the biophysical properties of mitoBK$_{Ca}$ in rat cardiac mitoplasts by exposing excised inside-out patches to symmetric bath and pipette solutions (150 $KMeSO_3$ and 5 μM Ca^{2+}). Transitions from closed (c) to open state (o) are the upward and downward deflections of the current recordings at positive and negative membrane potentials, respectively (Fig. 2A–C). MitoBK$_{Ca}$ P_o increased with membrane depolarization: the normalized NP_o versus membrane potential plot shows a half activation membrane potential ($V_{1/2}$) ~−55 mV at 12 μM matrix Ca^{2+} (P_o = 0.8 ± 0.05, n=5, Fig. 2A, D). The Ca^{2+}-dependence of mitoBK$_{Ca}$ channel, was evident from the progressive shift of the voltage dependent activation curve towards more depolarized potentials when matrix Ca^{2+} was reduced to 5 and 0.02 μM ($V_{1/2}$= +42 mV, and +70 mV, respectively, Fig. 2D). The apparent mitoBK$_{Ca}$ Ca^{2+} affinity was estimated by fitting the average P_o (n=4) at 3 different matrix Ca^{2+} and constant voltage (+20 mV) to a Hill function, yielding a $K_{1/2}$ = 8 μM and a Hill coefficient n_H = 2. MitoBK$_{Ca}$ displays a unitary conductance of 308 ± 19 pS (n=11) (Fig. 2E).

Paxilline inhibits the cardiac mitoBK$_{Ca}$ channel by stabilizing its closed state.

To confirm the identity of this large K^+ conductance as BK$_{Ca}$ channel, we used paxilline, a specific BK$_{Ca}$ blocker (Sanchez & McManus, 1996); 100 nM paxilline applied to the matrix side of inside-out patches exposed to 5 μM matrix Ca^{2+} decreased the P_o of the channel from 0.7 ± 0.1 to 0.2 ± 0.1 in <5 minutes (n=3) (Fig. 3A–D). The mean open time of the channel (7.2 ms ± 2.4 ms, control) did not change significantly in presence of paxilline (4.6 ms ± 1.2 ms) $p>0.05$, n=3, whereas the mean closed time augmented significantly from 3.8 ms ± 0.5 ms to 27 ms ± 0.4 ms (Fig. 3E–F, n=3, $p<0.05$). Thus, paxilline reduced the P_o of the channel mainly by stabilizing its closed state, a kinetic effect that has been previously reported for the plasma membrane BK$_{Ca}$ channel (Zhou & Lingle, 2014). Later, we used paxilline as a pharmacological tool to evaluate the physiological role of mitoBK$_{Ca}$ in mitochondrial Ca^{+2}-retention capacity.

MitoBK$_{Ca}$ functionally interacts with its auxiliary BK-β1 subunit; the activity of mitoBK$_{Ca}$ channel was negligible in the BK-β1 KO mice.

Figure 4A shows the immunoprecipitation of BK$_{Ca}$ alpha and the successful co-immunoprecipitation of BK-β1 subunit from cardiac mitochondrial lysate with a specific antibody against BK$_{Ca}$ alpha (see methods). Both subunits were also detected in the pre-immune mitochondrial fraction (input) as well as in the whole heart lysate. While the mitochondrial protein GRIM19 was also detected in both whole lysate and in the input, we found no signal in the IP product, indicating specificity of the association between BK-β1 subunit and BK$_{Ca}$. SERCA was used as a negative control and to discard cross-contamination of our mitochondrial fraction with membranes from the sarcoplasmic reticulum (SR). These results indicate that BK$_{Ca}$ channel interacts with its regulatory β1-subunit in cardiac mitochondria. To test how the interaction of mitoBK$_{Ca}$ with its regulatory

β1-subunit affects the biophysical properties of mitoBK$_{Ca}$ we characterize this channel in cardiac Wt mitochondria and in mitochondria from the β1 KO mice.

MitoBK$_{Ca}$ from Wt hearts displays a high P_o in 100% of the patches at all the membrane potentials tested (Fig. 4B–E). Interestingly, the activity of mitoBK$_{Ca}$ channel was negligible in mitochondria from the BK-β1 KO mice, where the channel was observed in only 5 patches from a total of 28 experiments (Fig. 4C). The remaining mitoBK$_{Ca}$ observed in the BK-β1 KO displayed the same slope conductance (~300 pS, Fig. 4D) as that of Wt mitoBK$_{Ca}$, but with a more depolarized voltage-dependence of activation ($V_{1/2}$= +47 mV at 12 μM matrix Ca^{2+}, n=4) (Fig. 4E). MitoBK$_{Ca}$ from the Wt displayed a Ca^{2+}-dependency similar to that observed in rat cardiac mitochondria (P_o~0.6, at +60 mV in 5 μM matrix Ca^{2+}, n=3, to P_o ~0.9, n=3 in 12 μM matrix Ca^{2+}) (Fig. 3). In addition, murine mitoBK$_{Ca}$ showed also sensitivity to paxilline, that reduced the P_o of the channel from 0.6 (n=3) (Fig. 5A and C) to 0.1 (n=3) (Fig. 5B and D) in 5 μM matrix Ca^{2+} at +20 mV. The blocking effect of paxilline was partially reduced by washing the patches with bath solution (P_o=0.4, n=3) (Fig. 5E and F).

Co-expression of regulatory BK-β1 subunit increases targeting of BKDEC to the mitochondria in HeLa cells.

The low P_o and the rare frequency in which mitoBK$_{Ca}$ channel was observed in the BK-β1 KO (Fig. 4B) suggests a reduction in the number of channels expressed and or properly targeted to the mitochondria in this genotype. Interestingly, the level of BK$_{Ca}$ transcript was significantly elevated in the BK-β1 KO, compared to Wt mice (GADPH served as a control of expression, see Methods). To test whether auxiliary BK-β1 subunits are required to target BK$_{Ca}$ into the inner mitochondrial membrane, we co-transfected HeLa cells with both BKDEC (Singh *et al.*, 2013) and auxiliary β1 subunit. Figure 6A–D show confocal images from mitochondria of HeLa cells co-expressing BKDEC and BK-β1 subunit. Panel A shows Mitotracker red signal (DAPI is in blue), panel B the BKDEC (green), panel C represents the signal of BK-β1 (blue). Panel D represents the merge of the four signals, white color indicates colocalization of BKDEC with BK-β1 and mitotracker red. E) Quantification of the co-localization index (Cci) relative to mitotracker red signal revealed that Cci was significantly higher in cells co-expressing BKDEC and BK-β1 subunit than those cells expressing only BKDEC.

Inhibition of mitoBK$_{Ca}$ reduces mitochondrial Ca^{2+} retention capacity.

Following the characterization of the biophysical properties of the large conductance BK$_{Ca}$ channel in mitochondria from adult rodent cardiomyocytes, we began to address its physiological role in mitochondria. Recent observations indicate that pharmacological opening of mitoBK$_{Ca}$ enhanced mitochondrial Ca^{2+} retention capacity (mCRC) (Sato *et al.*, 2005; Stowe *et al.*, 2006; Singh *et al.*, 2013). We measured mCRC in presence of paxilline as a way to investigate the effect that mitoBK$_{Ca}$ inhibition has on mitochondrial Ca^{2+} handling. Figures 7A and B show representative mCRC experiments, where the upward deflections in the fluorescence (Ca^{2+} green) recordings report Ca^{2+} elevations, caused by Ca^{2+} addition to the extra mitochondrial media (upward arrows) and by the release of Ca^{2+} from mitochondria; downward deflection represents mitochondrial Ca^{2+} uptake. Freshly isolated

cardiac mitochondria were challenged with pulses of 10 nmol $CaCl_2$ (Fig. 7A, arrows). Wt mitochondria were able to handle ~22 Ca^{2+} pulses before opening of the mitochondrial transition pore (mPTP) (Bopassa *et al.*, 2010; Singh *et al.*, 2013), due to mitochondrial Ca^{2+} overload (Fig. 7A, green line). Pre-incubation of mitochondria with 10 μM paxilline caused a significant reduction of mCRC, where ~15 pulses of $CaCl_2$ were sufficient to trigger the opening of mPTP (Fig. 7A, red line). These data indicate that a reduction in the P_o of mitoBK$_{Ca}$ channel with paxilline reduced mCRC (711 ± 30 for control and 494 ± 26 nmol/μg mitochondrial protein for mitochondria treated with paxilline, n=7) (Fig. 7C). Notably, mCRC was also reduced in the BK-β1 KO (553 ± 58 nmol/μg protein nmol Ca^{2+}, Fig. 7B blue line, n=5) compared to the Wt (Fig. 7C). Together, this data indicates that opening of mitoBK$_{Ca}$ channel and expression of its regulatory BK-β1 subunit are necessary to maintain mitochondrial Ca^{2+} homeostasis in cardiac cells.

A second population of mitoBK$_{Ca}$ channels with low P_o in rat cardiac mitochondria.

This population of channels was present in about 40% of the inside-out patches (7 out of 18 membrane patches). These channels also display a large conductance for K^+ (284 ± 6 pS, n=7 patches from 5 hearts) (Fig. 8A, D) and a $V_{1/2}$ = +42 mV in 12 μM matrix Ca^{2+} (n=4, Fig. 8C). The P_o of this channel was reduced when matrix [Ca^{2+}] was decreased (n=3) (Fig. 8A–C). A full characterization of the biophysical properties of this second population of mitoBK$_{Ca}$ channel is required to elucidate its association with regulatory subunits.

Discussion

MitoBK$_{Ca}$ is a large conductance K^+ channel.

Single channel conductance of mitoBK$_{Ca}$ varies between different tissues and cell types (Singh et al., 2012; Balderas et al., 2015). Cardiac mitoBK$_{Ca}$ channel has a conductance ranging between 190–300 pS (Xu et al., 2002; Ohya et al., 2005; Soltysinska et al., 2014). Likewise, we reported that cardiac mitoBK$_{Ca}$ is a Ca^{2+} dependent, voltage and paxilline sensitive channel, with a conductance for K^+ of 300 pS. A recent report has shown a slightly smaller conductance (145 pS) for cardiac mitoBK$_{Ca}$ (Frankenreiter et al., 2017). Although a detailed analysis is necessary to explain the differences observed between different groups, including the present study, it is clear that heterogeneous conductances exist in cardiac mitochondrial inner membrane as recently demonstrated (Soltysinska et al., 2014), where a conductance of 190 pS was reported for mitoBK$_{Ca}$, among other conductances ranging from 60 to 370 pS. We observed that substitution of Cl^- ions in the recording solutions, as well as the use of low concentrations of paxilline (100 nM) helped to dissect the biophysical properties of cardiac mitoBK$_{Ca}$ channel as well as its pharmacological profile.

Activation of mitoBK$_{Ca}$ channel depends on its regulatory β1 subunit.

Cell function and survival rely on adequate mitochondrial function. Oxidative phosphorylation (OXPHOS), ATP synthesis and the formation and opening of the mitochondrial PTP, among others are physiological processes regulated by mitochondrial Ca^{2+}. Since the discovery of BK$_{Ca}$ channel at the inner mitochondrial membrane (Siemen et al., 1999), a considerable effort has been made to establish the biophysical properties as well as the molecular composition of BK$_{Ca}$ channel in mitochondria and its role in

cardioprotection (Singh et al., 2013; Balderas et al., 2015). Despite significant advances, the physiological conditions under which mitoBK$_{Ca}$ channel might be active in respiring mitochondria remains unknown. The opening of a large K^+ conductance such as mitoBK$_{Ca}$ channel, would rapidly depolarize the mitochondrial membrane potential ($\Delta\Psi m$), reducing the driving force for Ca^{2+}, thus modulating mitochondrial Ca^{2+} uptake. The relative depolarized $V_{1/2}$ of activation of mitoBK$_{Ca}$ ($V_{1/2}$=−55 mV at ~10 μM matrix Ca^{2+}) with respect to mitochondrial membrane potential made the P_o of this channel presumably negligible under mitochondrial steady-state conditions ($\Delta\psi_m$=−180 mV; $[Ca^{2+}]_{mit}$<200 nM; pH=7.2; etc.) The remarkable high P_o displayed by mitoBK$_{Ca}$ at both negative and positive membrane potentials is similar to that previously reported for mitoBK$_{Ca}$ from various tissues and cell types (Siemen *et al.*, 1999; Xu *et al.*, 2002; Fahanik-Babaei *et al.*, 2011). In addition, its relative hyperpolarized $V_{1/2}$ (Fig. 2) compared to that of the BK$_{Ca}$-α subunit expressed alone (Meera *et al.*, 1996; Tanaka *et al.*, 1997; Nimigean & Magleby, 1999; Brenner *et al.*, 2000; Bao & Cox, 2005; Sweet & Cox, 2009), together with the expression of regulatory BK-β1 subunits in cardiac mitochondria (Fig. 4A) (Ohya *et al.*, 2005; Bautista *et al.*, 2009), supports the hypothesis of a functional association between cardiac mitoBK$_{Ca}$ and its auxiliary BK-β1 subunit. It is clear that a combination of physiological regulatory elements, rise in matrix $[Ca^{2+}]$, are required to increase mitoBK$_{Ca}$ channel P_o in steady-state respiring mitochondria.

The activity of plasma membrane BK$_{Ca}$ is independently regulated by the co-assembly of different β (1, 2) subunits together with γ (1) subunits (Yan & Aldrich, 2010, 2012) (Gonzalez-Perez *et al.*, 2015), thus interactions of cardiac mitoBK$_{Ca}$ channels with different regulatory subunits, β and or γ, are likely to occur. The most recent subproteomal analysis developed by our group revealed the interaction of mitoBK$_{Ca}$ channel with ~150 different mitochondrial proteins (Zhang *et al.*, 2017), including outer membrane import proteins, TOM 22 and TOM 70; as well as proteins of the respiratory complex (Zhang *et al.*, 2017). The mitochondrial subproteome also revealed association of mitoBK$_{Ca}$ with the ADP/ATP carrier, ANT (Zhang *et al.*, 2017), a regulator of the mitochondrial PTP (Kokoszka *et al.*, 2016). Therefore, interactions of mitoBK$_{Ca}$ channels with mitochondrial proteins and complexes may confer novel biophysical properties within the same population of mitochondria.

Regulatory BK-β1 subunit targets and activates mitochondrial BK$_{Ca}$ channel.

Biophysical characterization demonstrated that the large conductance for K^+, voltage dependent, Ca^{2+} and paxilline sensitive mitoBK$_{Ca}$ channel is present in adult rodent cardiomyocytes (Figs. 2–6). We also demonstrate a molecular interaction of mitoBK$_{Ca}$ channel with its regulatory β1 subunit in adult cardiomyocytes (Fig. 4). The low P_o and the scarcity of mitoBK$_{Ca}$–containing membrane patches in the BK-β1 KO (5 patches with active channels, out of 28 patches) indicates that BK-β1 subunit is necessary to effectively target BK$_{Ca}$ to the mitochondria, as has been seen in other cell systems, where targeting of plasma membrane BK$_{Ca}$ depends on the level of expression of BK-β1 subunit (Toro *et al.*, 2006). We observed that co-expression of BKDEC with its regulatory β1 subunit targets more channels to the mitochondria (Fig. 6). We recently reported that BK$_{Ca}$ channel is delivered into mitochondria through its interaction with the TOM22 import system (Zhang *et al.*,

2017). Despite this novel information, the molecular details and how the regulatory BK-β1 subunit contributes to target BK_{Ca} channel to the mitochondria remains to be established.

With regard to the physiological role of mitoBK$_{Ca}$, it has been hypothesized that activation of this large conductance helps to modulate mitochondrial Ca^{2+} handling, the details of this mechanism remains unclear. Current models suggest that when open mitoBK$_{Ca}$ would rapidly depolarize the ΔΨm (Testai *et al.*, 2013), hence reducing the mitochondrial driving force for Ca^{2+}, preventing mitochondrial Ca^{2+} overload (Wang *et al.*, 2004; Ohya *et al.*, 2005; Aon *et al.*, 2010). Under this scenario, activation of mitoBK$_{Ca}$ contributes to mitochondrial Ca^{2+} handling, controlling indirectly the formation and opening of mPTP, an essential step for cell survival (Halestrap & Richardson, 2015). In agreement with this hypothesis, reduced mitoBK$_{Ca}$ channel activity caused by pharmacological inhibition with paxilline or by lack of its regulatory β1 subunit, derivate in loss of mitochondrial Ca^{2+} handling (Fig. 7). This evidence support the hypothesis that association of mitoBK$_{Ca}$ channel with its auxiliary BK-β1 subunit is essential to maintain mitochondrial Ca^{2+} homeostasis in cardiac cells.

It is worth to consider that mitoBK$_{Ca}$ might be associated with regulatory subunits other than β1, as suggested by the second population of mitoBK$_{Ca}$ found in this work (Fig. 8), displaying a depolarized voltage-sensitivity ($V_{1/2}$ = +47 mV at 12 μM matrix Ca^{2+}) (Meera *et al.*, 1996; Brenner *et al.*, 2000). Heterogeneous populations of mitoBK$_{Ca}$ and association with different auxiliary subunits would increase the modes of regulation and the therapeutic targets that modulate this channel in cardiac mitochondria.

Supplementary Material

Refer to Web version on PubMed Central for supplementary material.

Acknowledgements

We thank the members of the Olcese laboratory for many insightful discussions and the Microscopy Techniques Core at UCLA members Marianne Cilluffo for assistance with electron microscopy. We thank MBA. Hlne Zammarchi and BS. Anthony Balynas for their valuable comments on this paper.

Funding

This work was supported by NIH HL107418 (LT, ES, RO), 1R01HL134346 (RO), HL124070 and HL141353 (DC), UC MEXUS-CONACyT Postdoctoral Fellowship FE-13–248 (EB) and AHA-WSA 15POST22490015 (EB).

Abbreviations:

mitoBK$_{Ca}$	mitochondrial large conductance for K^+, voltage- and Ca^{2+}-activated channel
P_o	open probability
CRC	calcium retention capacity

References

Aon MA, Cortassa S, Wei AC, Grunnet M & O'Rourke B. (2010). Energetic performance is improved by specific activation of K+ fluxes through K(Ca) channels in heart mitochondria. Biochim Biophys Acta 1797, 71–80. [PubMed: 19744465]

Balderas E, Zhang J, Stefani E & Toro L. (2015). Mitochondrial BKCa channel. Front Physiol 6, 104. [PubMed: 25873902]

Bao L & Cox DH. (2005). Gating and ionic currents reveal how the BKCa channel's Ca2+ sensitivity is enhanced by its beta1 subunit. J Gen Physiol 126, 393–412. [PubMed: 16186565]

Barrett JN, Barrett EF & Dribin LB. (1981). Calcium-dependent slow potassium conductance in rat skeletal myotubes In press 82.

Bautista L, Castro MJ, Lopez-Barneo J & Castellano A. (2009). Hypoxia inducible factor-2alpha stabilization and maxi-K+ channel beta1-subunit gene repression by hypoxia in cardiac myocytes: role in preconditioning. Circ Res 104, 1364–1372. [PubMed: 19461047]

Bentzen BH, Andersen RW, Olesen SP, Grunnet M & Nardi A. (2010). Synthesis and characterisation of NS13558: a new important tool for addressing KCa1.1 channel function ex vivo. Naunyn Schmiedebergs Arch Pharmacol 381, 271–283. [PubMed: 19798481]

Berkefeld H, Fakler B & Schulte U. (2010). Ca2+-activated K+ channels: from protein complexes to function. Physiol Rev 90, 1437–1459. [PubMed: 20959620]

Bopassa JC, Eghbali M, Toro L & Stefani E. (2010). A novel estrogen receptor GPER inhibits mitochondria permeability transition pore opening and protects the heart against ischemia-reperfusion injury. Am J Physiol Heart Circ Physiol 298, H16–H23. [PubMed: 19880667]

Brayden JE & Nelson MT. (1992). Regulation of arterial tone by activation of calcium-dependent potassium channels. Science 256, 532–535. [PubMed: 1373909]

Brenner R, Jegla TJ, Wickenden A, Liu Y & Aldrich RW. (2000). Cloning and functional characterization of novel large conductance calcium-activated potassium channel beta subunits, hKCNMB3 and hKCNMB4. J Biol Chem 275, 6453–6461. [PubMed: 10692449]

Contreras GF, Castillo K, Enrique N, Carrasquel-Ursulaez W, Castillo JP, Milesi V, Neely A, Alvarez O, Ferreira G, Gonzalez C & Latorre R. (2013). A BK (Slo1) channel journey from molecule to physiology. Channels (Austin) 7.

Cui J, Yang H & Lee US. (2009a). Molecular mechanisms of BK channel activation. Cell Mol Life Sci 66, 852–875. [PubMed: 19099186]

Cui J, Yang H & Lee US. (2009b). Molecular mechanisms of BK channel activation. Cell Mol Life Sci 66, 852–875. [PubMed: 19099186]

Fahanik-Babaei J, Eliassi A & Saghiri R. (2011). How many types of large conductance Ca(+)(2)-activated potassium channels exist in brain mitochondrial inner membrane: evidence for a new mitochondrial large conductance Ca(2)(+)-activated potassium channel in brain mitochondria. Neuroscience 199, 125–132. [PubMed: 21996476]

Frankenreiter S, Bednarczyk P, Kniess A, Bork NI, Straubinger J, Koprowski P, Wrzosek A, Mohr E, Logan A, Murphy MP, Gawaz M, Krieg T, Szewczyk A, Nikolaev VO, Ruth P & Lukowski R. (2017). cGMP-Elevating Compounds and Ischemic Conditioning Provide Cardioprotection Against Ischemia and Reperfusion Injury via Cardiomyocyte-Specific BK Channels. Circulation 136, 2337–2355. [PubMed: 29051185]

Gonzalez-Perez V, Xia XM & Lingle CJ. (2015). Two classes of regulatory subunits coassemble in the same BK channel and independently regulate gating. Nat Commun 6, 8341. [PubMed: 26388335]

Grundy D. (2015). Principles and standards for reporting animal experiments in The Journal of Physiology and Experimental Physiology. J Physiol 593, 2547–2549. [PubMed: 26095019]

Halestrap AP & Richardson AP. (2015). The mitochondrial permeability transition: a current perspective on its identity and role in ischaemia/reperfusion injury. J Mol Cell Cardiol 78, 129–141. [PubMed: 25179911]

Hoshi T, Pantazis A & Olcese R. (2013). Transduction of voltage and Ca2+ signals by Slo1 BK channels. Physiology (Bethesda) 28, 172–189. [PubMed: 23636263]

Kokoszka JE, Waymire KG, Flierl A, Sweeney KM, Angelin A, MacGregor GR & Wallace DC. (2016). Deficiency in the mouse mitochondrial adenine nucleotide translocator isoform 2 gene is

associated with cardiac noncompaction. Biochim Biophys Acta 1857, 1203–1212. [PubMed: 27048932]

Lancaster B & Nicoll RA. (1987). Properties of two calcium-activated hyperpolarizations in rat hippocampal neurones. J Physiol 389, 187–203. [PubMed: 2445972]

Latorre R & Brauchi S. (2006). Large conductance Ca2+-activated K+ (BK) channel: activation by Ca2+ and voltage. Biol Res 39, 385–401. [PubMed: 17106573]

Latorre R, Castillo K, Carrasquel-Ursulaez W, Sepulveda RV, Gonzalez-Nilo F, Gonzalez C & Alvarez O. (2017). Molecular Determinants of BK Channel Functional Diversity and Functioning. Physiol Rev 97, 39–87. [PubMed: 27807200]

Latorre R, Morera FJ & Zaelzer C. (2010). Allosteric interactions and the modular nature of the voltage- and Ca2+-activated (BK) channel. J Physiol 588, 3141–3148. [PubMed: 20603335]

Latorre R, Oberhauser A, Labarca P & Alvarez O. (1989). Varieties of calcium-activated potassium channels. Annu Rev Physiol 51, 385–399. [PubMed: 2653189]

Latorre R, Vergara C & Hidalgo C. (1982). Reconstitution in planar lipid bilayers of a Ca2+-dependent K+ channel from transverse tubule membranes isolated from rabbit skeletal muscle. Proc Natl Acad Sci U S A 79, 805–809. [PubMed: 6278496]

Ledoux J, Werner ME, Brayden JE & Nelson MT. (2006). Calcium-activated potassium channels and the regulation of vascular tone. Physiology (Bethesda) 21, 69–78. [PubMed: 16443824]

Lee US & Cui J. (2010a). BK channel activation: structural and functional insights. Trends Neurosci

Lee US & Cui J. (2010b). BK channel activation: structural and functional insights. Trends Neurosci 33, 415–423. [PubMed: 20663573]

Li M, Tanaka Y, Alioua A, Wu Y, Lu R, Kundu P, Sanchez-Pastor E, Marijic J, Stefani E & Toro L. (2010). Thromboxane A2 receptor and MaxiK-channel intimate interaction supports channel trans-inhibition independent of G-protein activation. Proc Natl Acad Sci U S A 107, 19096–19101. [PubMed: 20959415]

Li M, Zhang Z, Koh H, Lu R, Jiang Z, Alioua A, Garcia-Valdes J, Stefani E & Toro L. (2013). The beta1-subunit of the MaxiK channel associates with the thromboxane A2 receptor and reduces thromboxane A2 functional effects. J Biol Chem 288, 3668–3677. [PubMed: 23255603]

Meera P, Wallner M, Jiang Z & Toro L. (1996). A calcium switch for the functional coupling between alpha (hslo) and beta subunits (Kv,cabeta) of maxi K channels. FEBS Lett 385, 127–128. [PubMed: 8641456]

Meredith AL, Wiler SW, Miller BH, Takahashi JS, Fodor AA, Ruby NF & Aldrich RW. (2006). BK calcium-activated potassium channels regulate circadian behavioral rhythms and pacemaker output. Nat Neurosci 9, 1041–1049. [PubMed: 16845385]

Nimigean CM & Magleby KL. (1999). The beta subunit increases the Ca2+ sensitivity of large conductance Ca2+-activated potassium channels by retaining the gating in the bursting states. J Gen Physiol 113, 425–440. [PubMed: 10051518]

Ohya S, Kuwata Y, Sakamoto K, Muraki K & Imaizumi Y. (2005). Cardioprotective effects of estradiol include the activation of large-conductance Ca(2+)-activated K(+) channels in cardiac mitochondria. Am J Physiol Heart Circ Physiol 289, H1635–1642. [PubMed: 16113069]

Salkoff L, Butler A, Ferreira G, Santi C & Wei A. (2006). High-conductance potassium channels of the SLO family. Nat Rev Neurosci 7, 921–931. [PubMed: 17115074]

Sanchez M & McManus OB. (1996). Paxilline inhibition of the alpha-subunit of the high-conductance calcium-activated potassium channel. Neuropharmacology 35, 963–968. [PubMed: 8938726]

Sato T, Saito T, Saegusa N & Nakaya H. (2005). Mitochondrial Ca2+-activated K+ channels in cardiac myocytes: a mechanism of the cardioprotective effect and modulation by protein kinase A. Circulation 111, 198–203. [PubMed: 15623543]

Siemen D, Loupatatzis C, Borecky J, Gulbins E & Lang F. (1999). Ca2+-activated K channel of the BK-type in the inner mitochondrial membrane of a human glioma cell line. Biochem Biophys Res Commun 257, 549–554. [PubMed: 10198249]

Singh H, Lu R, Bopassa JC, Meredith AL, Stefani E & Toro L. (2013). MitoBK(Ca) is encoded by the Kcnma1 gene, and a splicing sequence defines its mitochondrial location. Proc Natl Acad Sci U S A 110, 10836–10841. [PubMed: 23754429]

Singh H, Stefani E & Toro L. (2012). Intracellular BK(Ca) (iBK(Ca)) channels. J Physiol 590, 5937–5947. [PubMed: 22930268]

Soltysinska E, Bentzen BH, Barthmes M, Hattel H, Thrush AB, Harper ME, Qvortrup K, Larsen FJ, Schiffer TA, Losa-Reyna J, Straubinger J, Kniess A, Thomsen MB, Bruggemann A, Fenske S, Biel M, Ruth P, Wahl-Schott C, Boushel RC, Olesen SP & Lukowski R. (2014). KCNMA1 encoded cardiac BK channels afford protection against ischemia-reperfusion injury. PLoS One 9, e103402. [PubMed: 25072914]

Stowe DF, Aldakkak M, Camara AK, Riess ML, Heinen A, Varadarajan SG & Jiang MT. (2006). Cardiac mitochondrial preconditioning by Big Ca2+-sensitive K+ channel opening requires superoxide radical generation. Am J Physiol Heart Circ Physiol 290, H434–H440. [PubMed: 16126810]

Sweet TB & Cox DH. (2009). Measuring the influence of the BKCa {beta}1 subunit on Ca2+ binding to the BKCa channel. J Gen Physiol 133, 139–150. [PubMed: 19139175]

Tanaka Y, Meera P, Song M, Knaus H-G & Toro L. (1997). Molecular constituents of maxi K_{Ca} channels in human coronary smooth muscle. Predominant α + β subunit complexes. J Physiol 502, 545–557. [PubMed: 9279807]

Testai L, Martelli A, Marino A, D'Antongiovanni V, Ciregia F, Giusti L, Lucacchini A, Chericoni S, Breschi MC & Calderone V. (2013). The activation of mitochondrial BK potassium channels contributes to the protective effects of naringenin against myocardial ischemia/reperfusion injury. Biochem Pharmacol 85, 1634–1643. [PubMed: 23567997]

Toro B, Cox N, Wilson RJ, Garrido-Sanabria E, Stefani E, Toro L & Zarei MM. (2006). KCNMB1 regulates surface expression of a voltage and Ca2+-activated K+ channel via endocytic trafficking signals. Neuroscience 142, 661–669. [PubMed: 16908104]

Wang X, Yin C, Xi L & Kukreja RC. (2004). Opening of Ca2+-activated K+ channels triggers early and delayed preconditioning against I/R injury independent of NOS in mice. Am J Physiol Heart Circ Physiol 287, H2070–2077. [PubMed: 15217801]

Wu Y, Eghbali M, Ou J, Lu R, Toro L & Stefani E. (2010). Quantitative determination of spatial protein-protein correlations in fluorescence confocal microscopy. Biophys J 98, 493–504. [PubMed: 20141764]

Xu W, Liu Y, Wang S, McDonald T, Van Eyk JE, Sidor A & O'Rourke B. (2002). Cytoprotective role of Ca2+- activated K+ channels in the cardiac inner mitochondrial membrane. Science 298, 1029–1033. [PubMed: 12411707]

Yan J & Aldrich RW. (2010). LRRC26 auxiliary protein allows BK channel activation at resting voltage without calcium. Nature 466, 513–516. [PubMed: 20613726]

Yan J & Aldrich RW. (2012). BK potassium channel modulation by leucine-rich repeat-containing proteins. Proc Natl Acad Sci U S A 109, 7917–7922. [PubMed: 22547800]

Zhang J, Li M, Zhang Z, Zhu R, Olcese R, Stefani E & Toro L. (2017). The mitochondrial BKCa channel cardiac interactome reveals BKCa association with the mitochondrial import receptor subunit Tom22, and the adenine nucleotide translocator. Mitochondrion 33, 84–101. [PubMed: 27592226]

Zhou Y & Lingle CJ. (2014). Paxilline inhibits BK channels by an almost exclusively closed-channel block mechanism. J Gen Physiol 144, 415–440. [PubMed: 25348413]

Key Points

- Association of plasma membrane BK_{Ca} channels with BK-β subunits shape their biophysical properties and physiological roles; however, functional modulation of mitochondrial BK_{Ca} channel (mitoBK_{Ca}) by BK-β subunits is not established.
- MitoBK_{Ca}-α, and regulatory BK-β1 subunit associate in mouse cardiac mitochondria.
- A large fraction of mitoBK_{Ca} displayed properties similar to that of plasma membrane BK_{Ca} when associated with BK-β1 (left-shifted voltage dependence of activation, $V_{1/2}$=−55mV, 12 μM matrix Ca^{2+}).
- In the BK-β1 KO mice, cardiac mitoBK_{Ca} displayed low P_o and depolarized $V_{1/2}$ of activation (+47mV at 12 μM matrix Ca^{2+})
- Co-expression of BK_{Ca} with BK-β1 subunit in HeLa cells doubled the density of BK_{Ca} in mitochondria.
- This work supports the view that cardiac mitoBK_{Ca} channel is functionally modulated by the BK-β1 subunit; proper targeting and activation of mitoBK_{Ca} shapes mitochondrial Ca^{2+} handling.

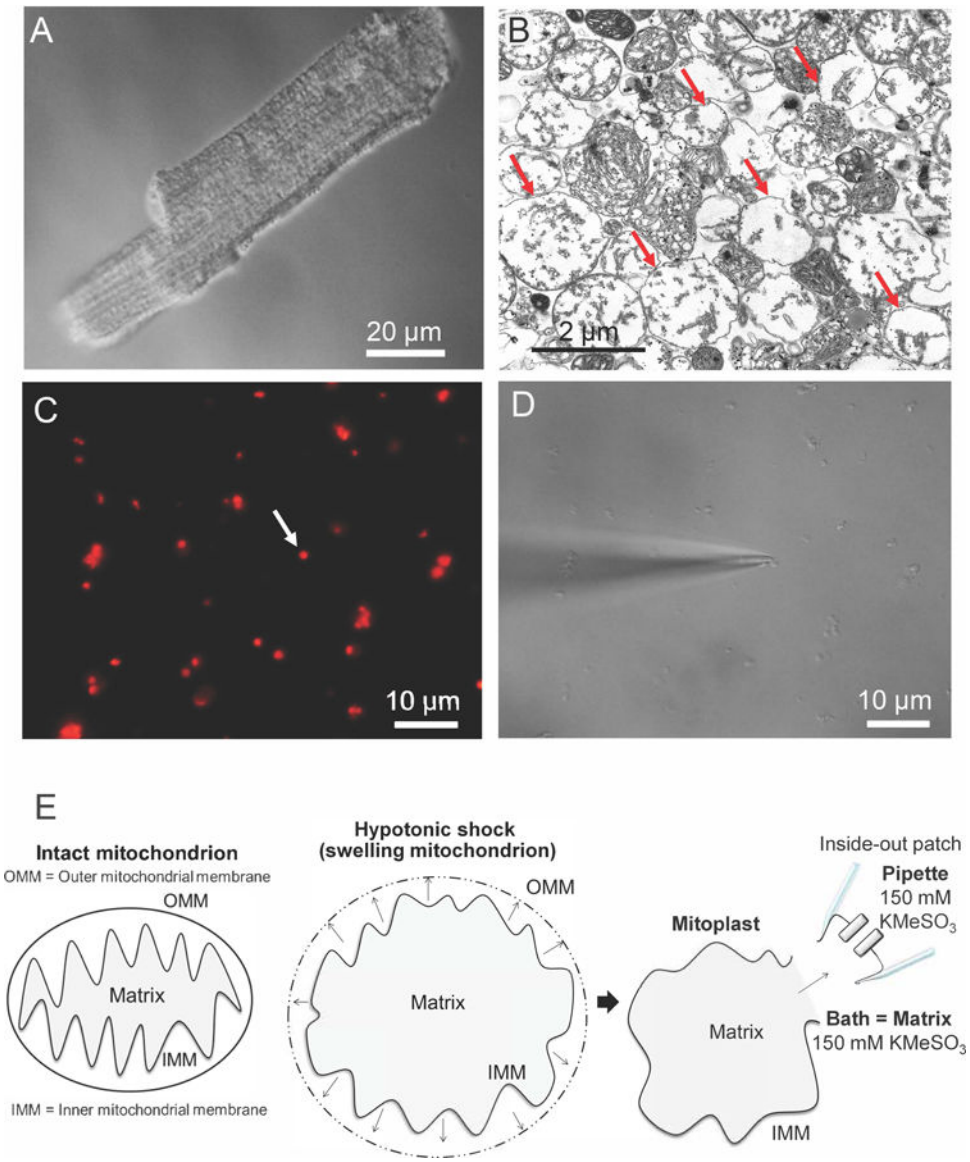

Figure 1. Preparation of mitoplast from left ventricle cardiomyocytes

A) Healthy rat cardiomyocytes isolated with a Langendorff perfusion apparatus. B) Electron microscopy image of mitoplasts (inner mitochondrial membrane devoid of outer membrane), red arrow. A low percentage of intact swollen mitochondria remained (top-left panel B). C) Mitoplasts labeled with Mitotracker Red visualized with differential interference contrast (DIC) Nomarski microscopy through a 60X objective. The arrow in C indicate a selected mitoplast for patch-clamp. D) DIC image of panel C show a borosilicate patch pipette next to a mitoplast. E) Schematic representation of the preparation of mitoplasts. In an excised patch (inside-out configuration), the bath solution represents the mitochondrial matrix.

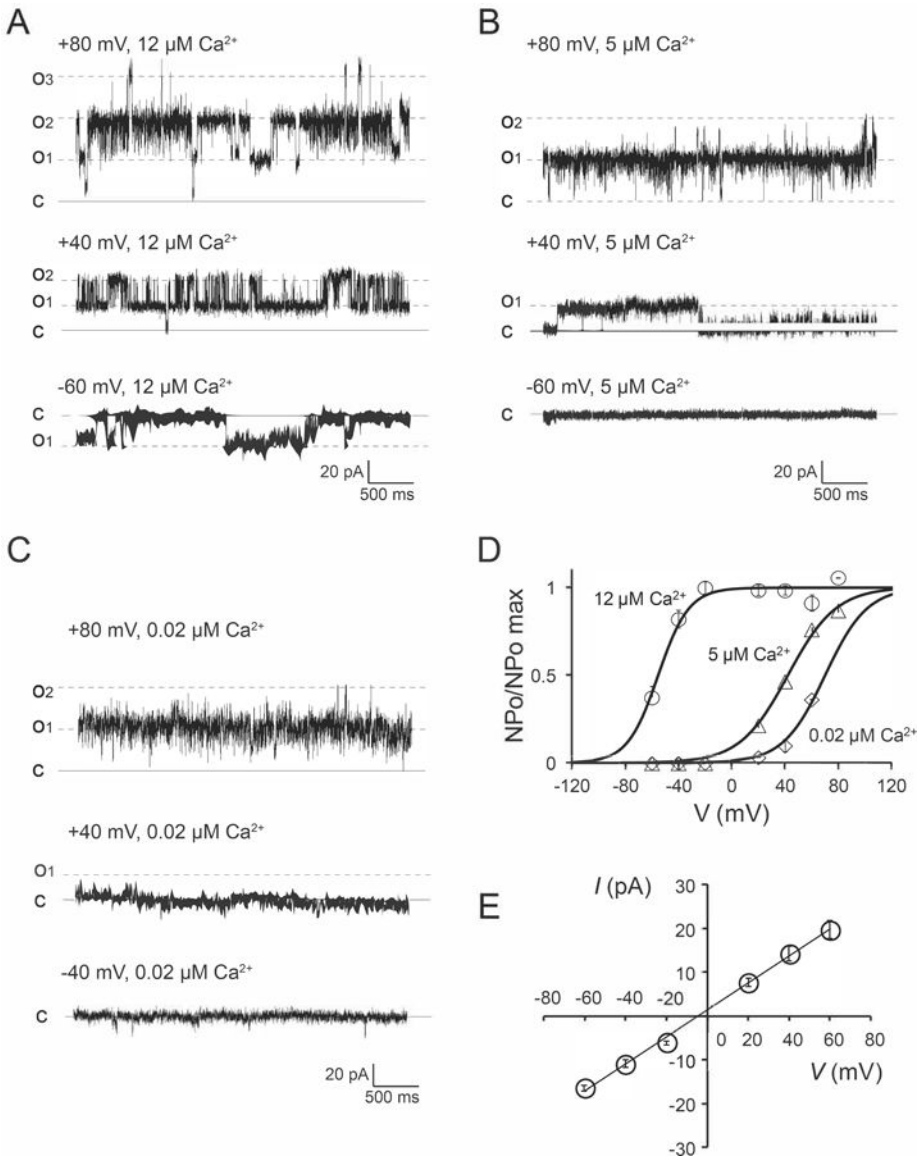

Figure 2. Voltage-dependence of MitoBK$_{Ca}$ channel.

In an excised inside-out patch, the bath solution represents the matrix side of the mitoplast. Channel activity was recorded in symmetric 150 KMeSO$_4$. A) Single channel currents from a patch that contains at least three channels obtained at 12 μM matrix Ca^{2+} (c=closed state; o=open state). B) The same patch as in A exposed to 5 μM matrix Ca^{2+}. Recordings in B show the activity of only one channel at positive membrane potentials. C) Same patch as in A and B exposed to 0.02 μM matrix Ca^{2+}, single channel current was observed only at +80 mV. D) Plot of normalized NP_o vs V. Data points were fit to a Boltzmann distribution (continuous lines) with a $V_{1/2}$=−55, +42 and +70 mV at 12 (n=8), 5 (n=4), and 0.02 μM Ca^{2+} (n=3), respectively. Z values of 2.2, 1.4 and 1.6 were calculated for 12, 5 and 0.02 μM matrix Ca^{2+}, respectively. E) Plots of I vs. V of mitoBK$_{Ca}$ channels with a slope conductance of 309±19 pS (n=11). Bars represent mean and SEM here and throughout.

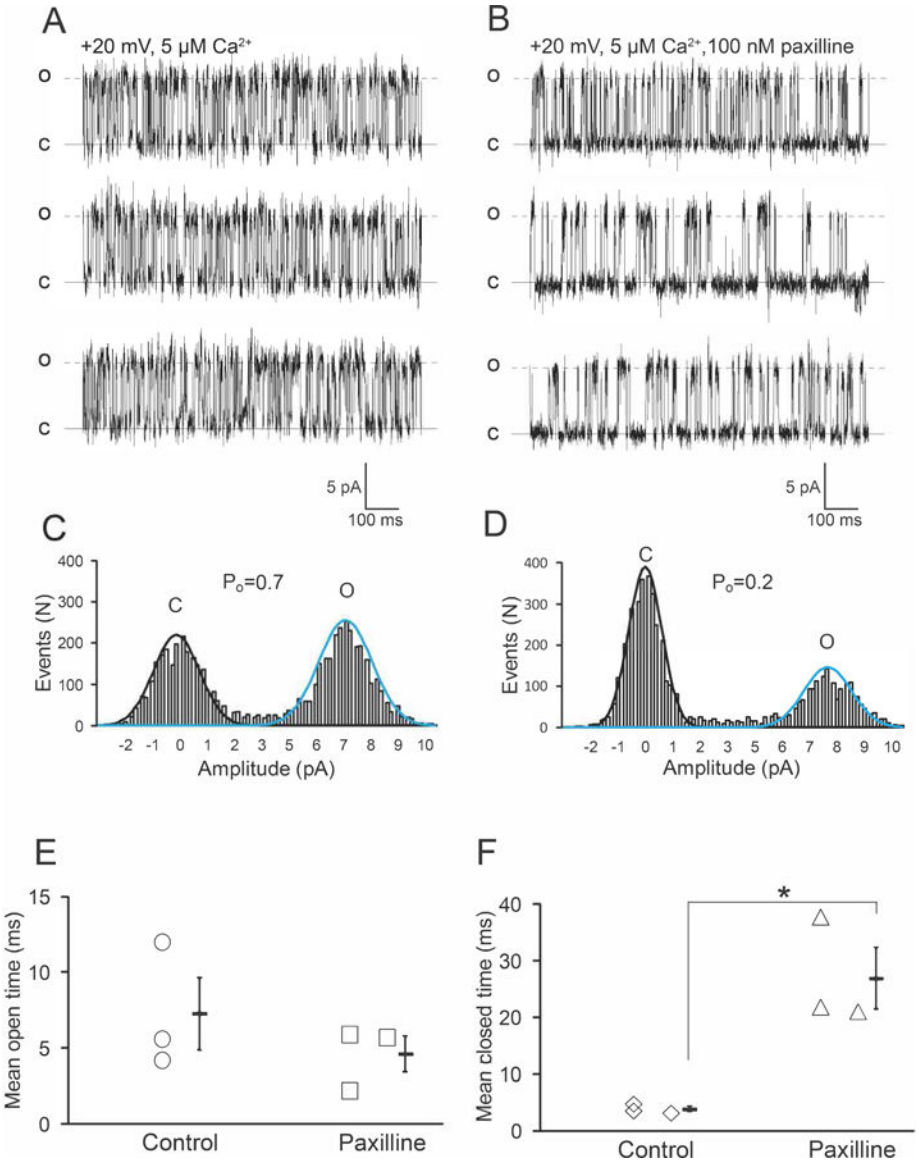

Figure 3. Paxilline reduces the open probability of mitoBK$_{Ca}$ channels.

Single-channel currents of mitoBK$_{Ca}$ recorded from the same mitoplast in absence (A) and in presence of paxilline (B) at the indicated matrix Ca^{2+} and membrane potential. Paxilline decreased the P_o of the 7 pA channel from 0.77±0.1 to 0.41±0.1 (n=3) as indicated in the current amplitude histograms (C and D). Mean open time (E) and mean closed time (F) observed in 3 different patches. Paxilline augmented significantly the mean closed time of the channel (*p<0.05 Student's t-test, n=3 hearts).

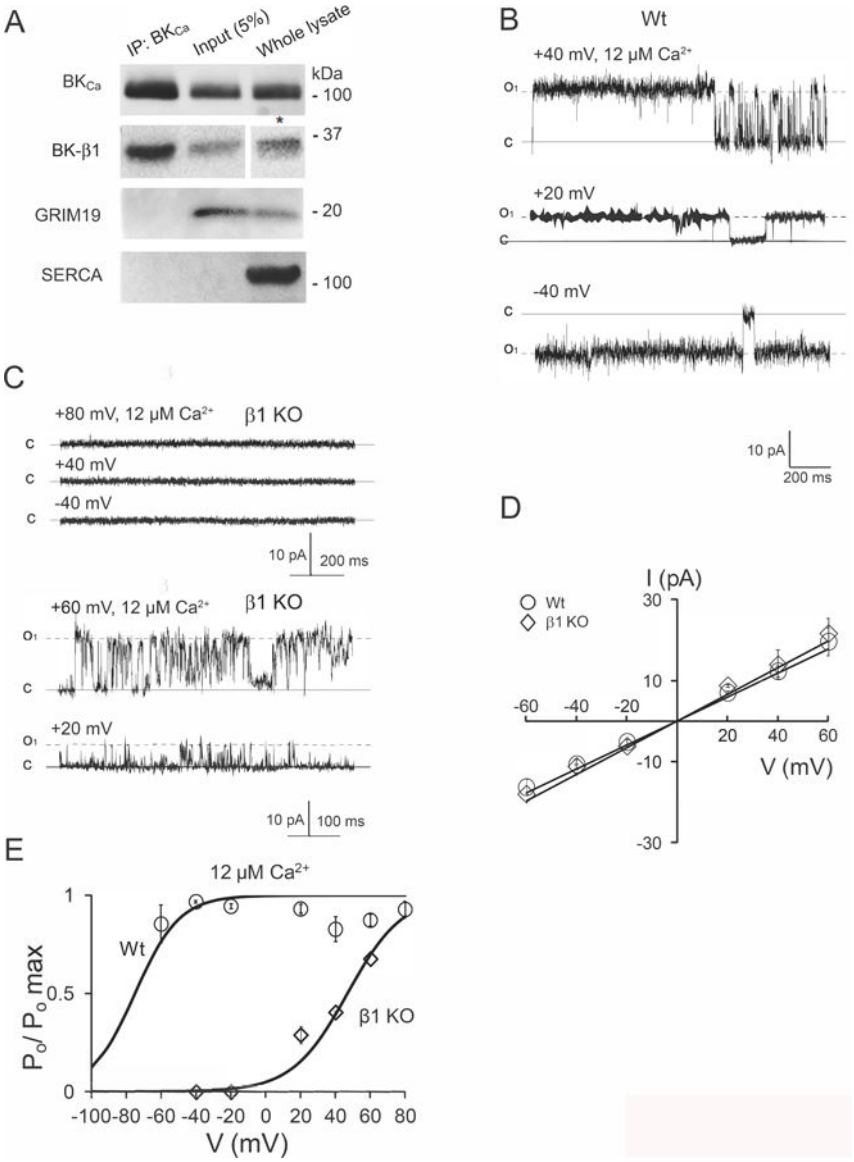

Figure 4. MitoBK$_{Ca}$ alpha and auxiliary β1 subunit association in cardiac mitochondria.

A) Immunoprecipitation (IP) of BK$_{Ca}$ alpha and BK-β1 subunit with an antibody against BK$_{Ca}$ alpha (see methods). Western blots revealed the presence of GRIM 19 and SERCA as markers of mitochondrial and sarcoplasmic reticulum membranes (4A, lower panels). *The signal of BK-β1 in the whole lysate was detected with chemiluminescent (ECL) substrate Supersignal™ West Femto Maximun sensitivity (see methods). Taken together, these results indicates an association between mitoBK$_{Ca}$ and its auxiliary β1 subunit. Having demonstrated this, we characterized the biophysical properties of mitoBK$_{Ca}$ in Wt and β1-KO cardiac mitoplasts. B) Single-channel currents of mitoBK$_{Ca}$ recorded from Wt mitoplasts. The P_o of the channel was 0.9 ± 0.08, n=4, in average at +80 mV and the indicated matrix Ca^{2+}. C) Representative traces of a mitoplast from the β1 KO, were no single-channel current was detected at the indicated voltages and matrix Ca^{2+} (upper traces). Few mitoplasts (5 out of 28, mitoplasts, n=5 hearts) showed mitoBK$_{Ca}$ channel activity with

a P_o of 0.4 ± 0.004, n=3 at +40 mV in the indicated matrix Ca^{2+}. D) Plots of I vs. V at 12 μM matrix Ca^{2+} from Wt and β1 KO mitoplasts (data from 6 and 3 patches, respectively). A slope conductance of 302±26 (n=4) and 335 ±15 pS (n=3) was calculated for Wt and β1 KO, respectively. E) Plots of P_o vs. V for mitoBK_{Ca} channels, data points represent the average of 4 and 3 mitoplasts for Wt and BK-β1 KO, respectively. Bars SEM.

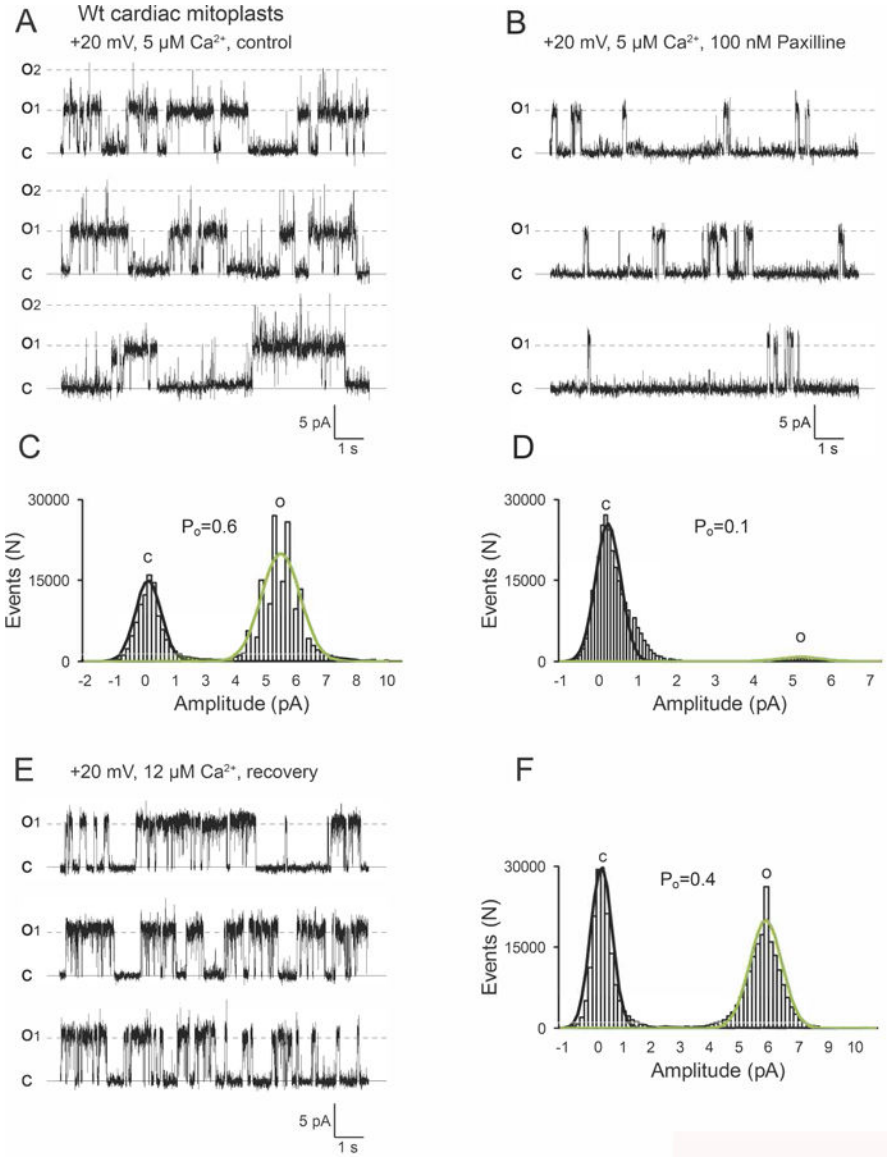

Figure 5. Paxilline reversibly blocks mouse cardiac mitoBK$_{Ca}$ channel

Single channel current in absence (A) and in presence (B) of paxilline at the indicated voltage and matrix Ca^{2+}. C) Current amplitude histogram of the 6 pA channel recorded in A, paxilline reduced the P_o from 0.7±0.1 to 0.2±0.09 (n=3) (D). E) Single channel current recorded after the patch was perfused again with 12 μM matrix Ca^{2+}. F) Current amplitude histogram that shows the reappearance of the 6 pA current (P_o=0.4) after washing out paxilline.

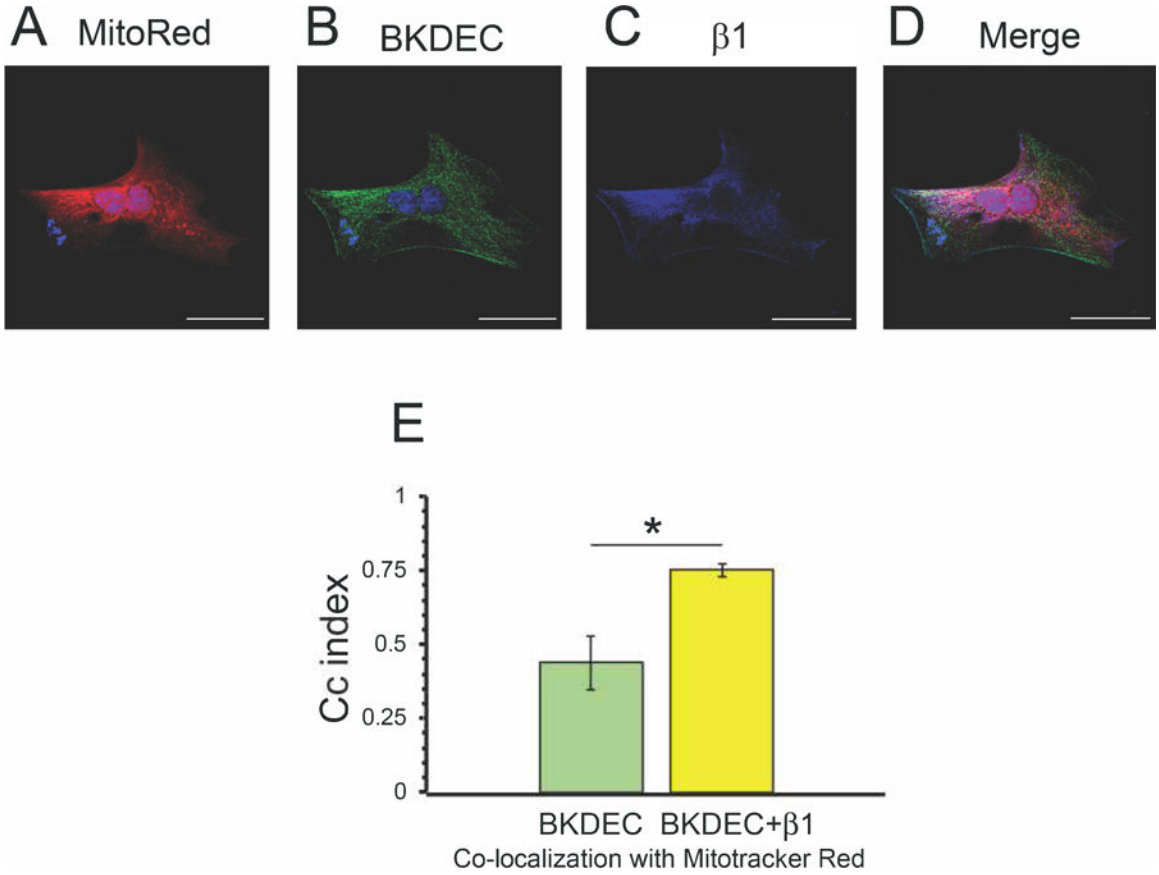

Figure 6. Localization of BKDEC and β1 subunit in HeLa cells.

A) Cultured cells co-transfected with BKDEC alpha+β1subunit, loaded with mitotracker red, and DAPI B) β1-flag labeled with an anti-flag C) BKDEC labeled with anti-HA. D) Merge of mitotracker red, BKDEC and β1. E) Cross-correlation index (CCi), relative to mitotracker red signal, calculated from cells overexpressing BKDEC alone (Cci=0.53±0.05) and co-expressed with β1 subunit (Cci=0.77±0.01, n=11 cells from 3 different preparations).*p<0.05.

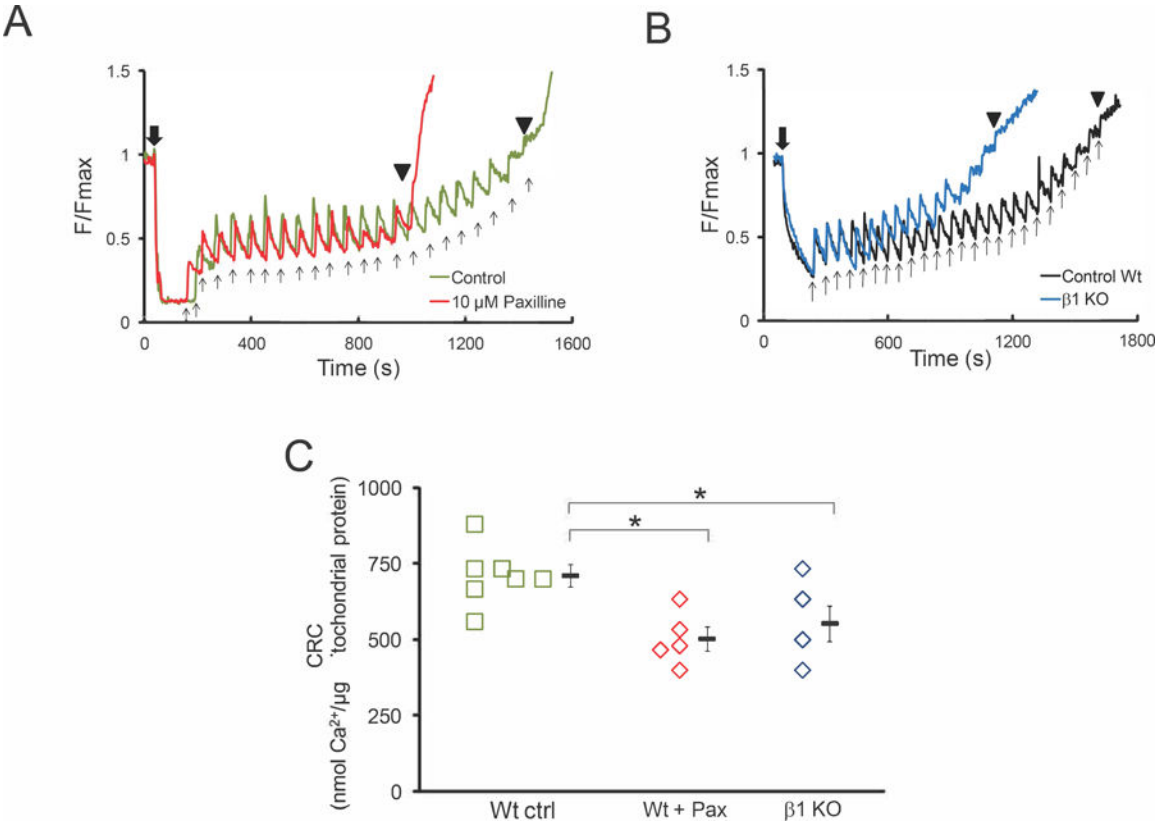

Figure 7. Mitochondrial calcium uptake is impaired by Paxilline and by genetic ablation of β1-subunit

A) Paxilline reduces the amount of mitochondrial Ca^{2+} necessary to induce formation and opening of mPTP. B) Mitochondria from the β1 KO required less Ca^{2+} than mitochondria from the Wt to trigger the opening of mPTP. C) Calcium retention capacity values obtained in A for paxilline and in B for the β1-KO mitochondria. Bars SEM, (*p<0.05 Student's t-test). Black downward arrow, addition of mitochondria. Black upward arrows, 10 nmol $CaCl_2$ pulses. (▼) opening of mPTP.

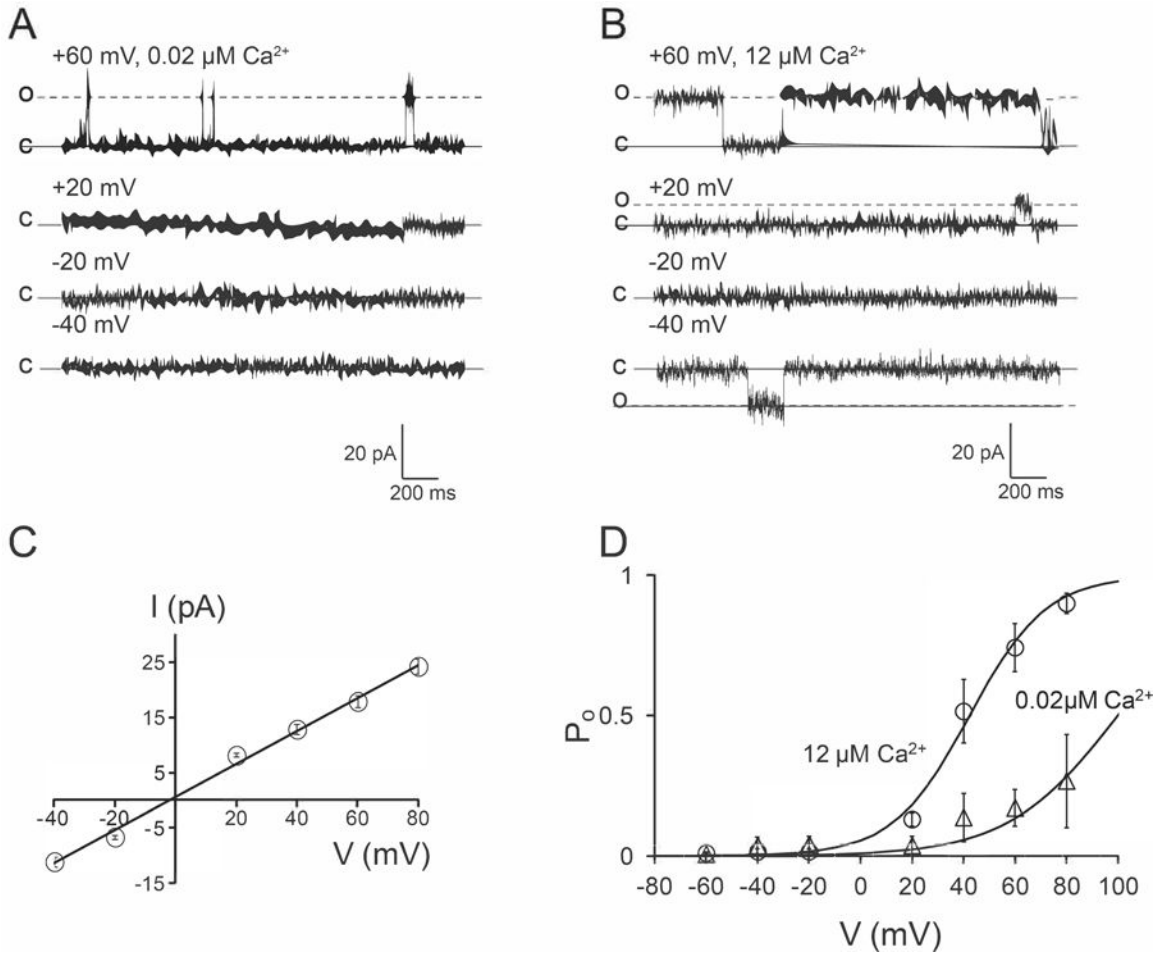

Figure 8. A different population of mitoBK$_{Ca}$ in cardiac mitochondria

A) Single channel currents recorded in 0.02 μM matrix Ca^{2+} at the indicated voltages. B) Same patch as in A exposed to 12 μM matrix Ca^{2+}. C) Plot of *I* vs. *V*, a slope conductance of 284 ± 6 pS (n=7) was calculated. D) Plots of P_o vs. *V* from the currents observed in A and B, data points represent an average of ≥4 different patches at the indicated matrix Ca^{2+}.

Table 1.

Quantitative PCR primers

Accession number	Primers	Sequence
MaxiK U40603 (alpha subunit)	Forward Reverse	5’ -TACTTCAATGACAATATCCTCACCCT-3’ 5’ -ACCATAACAACCACCATCCCCTAAG-3’
MaxiK AF020712 (β1 subunit)	Forward Reverse	5’ -GTATCACACAGAAGACACTCGGGA-3’ 5’ -AAGAAGGAGAAGAGGAGGATTTGGG-3’
GAPDH	Forward Reverse	5’-AGGTCGGTGTGAACGGATTTG-3’ 5’-TGTAGACCATGTAGTTGAGGTCA-3’